Pergamon

*Biochemical Pharmacology*, Vol. 48, No. 2, pp. 361–370, 1994.

0006-2952/94 $7.00 + 0.00

0006-2952(94)E0152-B

# MECHANISM OF THE SELECTIVE HYPOXIC CYTOTOXICITY OF 1-METHYL-2-NITROIMIDAZOLE

CHRISTINE B. BREZDEN,*†‡ ROBERT A. MCCLELLAND§ and A. MICHAEL RAUTH*†

*Division of Experimental Therapeutics, The Ontario Cancer Institute, Toronto; and Departments of †Medical Biophysics and §Chemistry, University of Toronto, Toronto, Canada

(*Received* 16 *December* 1993; *accepted* 4 *March* 1994)

**Abstract**—2-Nitroimidazoles were introduced into radiation therapy to test their ability to radiosensitize hypoxic cells in solid human tumours. In addition, they are selectively reduced in hypoxic cells to form reactive metabolites that may be effective cytotoxins. 1-Methyl-2-nitroimidazole ($INO_2$) was investigated as a model compound to study the mechanism of selective bioreduction in hypoxic cells. Results demonstrated that $INO_2$ was toxic under hypoxic conditions (tested via colony-forming assay) at concentrations where no toxicity was observed for aerobic cells. This selective hypoxic toxicity was a function of both concentration and time. The depletion of both glutathione and protein thiols occurred under hypoxic conditions and preceded a rise in intracellular calcium levels. Previous work with INO, the nitroso intermediate of $INO_2$ reduction, also showed concentration-dependent cytotoxicity, and glutathione and protein thiol depletion, which was followed by an increase in intracellular calcium levels. The kinetics of cytotoxicity and cellular reactions were slower for the parent compound, $INO_2$, as compared with the $2e^-$ reductive metabolite, INO, reflecting the limited enzymatic production of the reactive intermediate in the $INO_2$ experiments. Zeiosis (membrane blebbing) and chromatin condensation occurred shortly after treatment of cells with equitoxic concentrations of both $INO_2$ (under hypoxic conditions) and INO (under aerobic conditions), suggesting that an apoptotic-like death mechanism may be involved. However, analysis of DNA isolated from both $INO_2$- and INO-treated cells, up to 2 hr after treatment, did not reveal any nucleosomal fragmentation, another characteristic feature of cells undergoing apoptosis. The toxicity of high $INO_2$ concentrations toward CHO cells is consistent with the production of an INO intermediate and has several features characteristic of an apoptotic mechanism of cell death.

It is well documented that some solid human tumours contain regions of low oxygen tension, and cells in these hypoxic regions may limit the tumouricidal effects of ionizing radiation compared with their aerobic counterparts [1]. Introduction of electron-affinic compounds such as 2-nitroimidazoles as adjuncts to radiotherapy showed some therapeutic benefit clinically. However, dose-limiting neurotoxicity was experienced in patients [2, 3]. Clinical Phase II and Phase III trials have been carried out and are currently in progress using combinations of 2-nitroimidazole analogues with radiotherapy [4, 5]. In addition to their use as radiosensitizers, 2-nitroimidazoles are also preferentially toxic to hypoxic cells. This selective hypoxic cytotoxicity is due to the generation of reactive toxic species via cellular bioreductive metabolism of the nitro moiety of the 2-nitroimidazole compound. Moreover, this selective hypoxic bioreduction has stimulated the use of radiolabelled 2-nitroimidazoles for imaging tumour hypoxia, thereby allowing for more effective treatment regimens to be administered [6, 7].

Although bioreduction of 2-nitroimidazoles results in hypoxic cell toxicity, uncertainty as to the cytotoxic intermediate(s) and its cellular targets still remains. The 4 electron ($e^-$) reduction product of MISO‖, the hydroxylamine, has been shown to react with protein and DNA [8, 9]. Further analysis demonstrated that the hydroxylamine was unstable at neutral physiological pH with a short half-life compared with its stability under acidic conditions [10]. However, the hydroxylamine was non-toxic when added to cellular systems [11]. By contrast, more recent studies have shown that the nitroso intermediate (INO) of $INO_2$, the $2e^-$ reduction product, is also highly reactive and cytotoxic to human and rodent cell lines [11, 12]. Furthermore, cellular incubation with INO demonstrated intracellular thiol depletion followed by a sustained elevation in intracellular calcium levels, which were lethal to the cell [13]. In these previous experiments, INO cellular testing was performed by adding the drug from outside the cells. Thus, it can be questioned to what degree these results model what occurs with $INO_2$, which is reduced enzymatically in the cell to form INO over a prolonged period of time under hypoxia.

To further evaluate the possible role of the INO intermediate of $INO_2$ as the toxic species involved in the selective hypoxic cytotoxicity of 2-nitro-

‡ Corresponding author: Christine B. Brezden, Ontario Cancer Institute, 500 Sherbourne St., Rm. 739, Toronto, Ontario, Canada M4X 1K9. Tel. (416) 924-0671, Ext. 4917; FAX (416) 926-6529.

‖ Abbreviations: MISO, misonidazole; $INO_2$, 1-methyl-2-nitroimidazole; INO, 1-methyl-2-nitrosoimidazole; CHO, Chinese hamster ovary; GSH, reduced glutathione; GSSG, oxidized glutathione; Pr-SH, protein sulfhydryls; α-MEM, Minimum Essential Medium; DTNB, 5,5′-dithiobis-(2-nitrobenzoic) acid; GR, glutathione reductase; NEM, *N*-ethylmaleimide; GT, guanidine thiocyanate; FBS, fetal bovine serum; IL-2, interleukin-2; and TCA, trichloroacetic acid.

imidazoles, the parent compound $INO_2$ was investigated. The toxicity of $INO_2$ to CHO cells was determined under hypoxic and aerobic conditions. The effect of $INO_2$ on intracellular glutathione, reduced (GSH) and oxidized (GSSG) forms, Pr-SH and intracellular calcium levels was determined and compared with previous results for INO at equitoxic drug levels. In addition, morphological effects of $INO_2$ and INO were determined using transmission and scanning electron microscopy, and DNA damage was assessed by gel electrophoresis. The results of these experiments are presented and discussed in terms of a possible mechanism of cell death by $INO_2$ that involves changes in the intracellular redox state [14] leading to an apoptotic-like cell death.

## MATERIALS AND METHODS

*Chemicals and reagents.* Both $INO_2$ and INO were synthesized by Dr. R. A. McClelland in the Department of Chemistry at the University of Toronto, and characterized as previously described [11, 15]. Stock solutions of $INO_2$ were prepared in PBS prior to each experiment. Concentrations were confirmed by diluting stocks and measuring drug absorbance using $\varepsilon_{320} = 8000$ [11]. INO was prepared as reported by Noss *et al.* [11], and concentrations were measured spectrophotometrically using $\varepsilon_{360} = 20{,}000$ prior to each experiment. For GSH and Pr-SH determination: GR, NADPH, NEM and DTNB were purchased from the Sigma Chemical Co., St. Louis, MO, U.S.A.; EDTA and SDS were obtained from GIBCO, Burlington, ON, Canada; HCl and TCA were purchased from Fisher Scientific, Toronto, ON, Canada. For $Ca^{2+}$ measurements: indo-1AM was purchased from Molecular Probes, Eugene, OR, U.S.A.; ionomycin was obtained from Boehringer Mannheim, Laval, PQ, Canada; and $MnCl_2$ and verapamil were from Sigma. For DNA gel electrophoresis: GT, Tris, 2-mercaptoethanol, ammonium acetate and Sarkosyl were purchased from Sigma; agarose, ethidium bromide and $\phi$x174RF DNA-*Hae* III (all ultra-pure grade) were purchased from GIBCO; glycogen, RNase and $\lambda$DNA-*Hind* III were purchased from Boehringer Mannheim. Glutaraldehyde, used for electron microscopy, was purchased from Morivac Laboratories, Halifax, NS, Canada.

*Cells.* Cells used for all experiments were the CHO cell subclone AA8-4, which was obtained originally from Dr. L. H. Thompson of Lawrence Livermore Laboratories, Livermore, CA, U.S.A. CHO cells were grown routinely in suspension culture at 37° in growth medium consisting of $\alpha$-MEM (Sigma) supplemented with 10% FBS (Whittaker Bioproducts Inc., Walkersville, MD, U.S.A.). Cell survival was measured following incubation of stirred suspension cultures (10 mL with a cell density of $10^6$ cells/mL) in 40 mL polyshell vials (John's Scientific Inc., Toronto, ON, Canada) with $INO_2$ at a constant concentration for varying lengths of time at 37° under aerobic conditions (95% air:5% $CO_2$) or hypoxic conditions (95% $N_2$:5% $CO_2$ <10 ppm $O_2$) (Gas Dynamics Inc., Toronto, ON, Canada) in $\alpha$-MEM plus 10% FBS. Aliquots were removed at specific times, diluted and plated in 5 mL of growth medium ($\alpha$-MEM plus 10% FBS) in tissue culture dishes (60 × 15 mm) (Falcon, Beckton Dickinson Labware, Lincoln Park, NJ, U.S.A.). After 8 days, plates were stained with methylene blue, and colonies consisting of 50 cells or more were scored and counted. Exposure of cells to INO was carried out as a function of drug concentration as previously described [11].

As a positive apoptotic control for DNA gel electrophoresis, cells from the murine cytotoxic T-lymphocyte cell line CTLL-2 (ATCC TIB 214) were grown routinely in flasks in growth medium consisting of HEPES-medium (Fisher) supplemented with 10% FBS and 50 $\mu$M murine IL-2 [16].

*GSH determination.* Total intracellular GSH (both GSH and GSSG) was measured using the procedure of Tietze [17] as modified by Bump *et al.* [18].

*Pr-SH assay.* Intracellular Pr-SH levels were measured using the procedure previously described by Albano *et al.* [19]. Briefly, 1-mL aliquots of $10^6$ cells/mL were removed from $INO_2$-treated stirred suspensions either under hypoxic or aerobic conditions at desired times. These aliquots were washed once in PBS and then resuspended in 0.5 mL PBS and 1 mL of 5% TCA–EDTA (1.5 mM). Samples were then vortexed lightly, left on ice for 30 min to allow for complete protein precipitation, and then microcentrifuged for 6 min at 8000 *g*; the pellet was resuspended in 3 mL of 0.1 M Tris–HCl buffer (containing 5 mM EDTA and 0.5% SDS, pH 8.6). The 3-mL volume was divided equally into 1-mL aliquots for Pr-SH determination: a 1-mL aliquot was reacted with 5 mM NEM followed by a 6 mM DTNB reaction to give a control value; the other two aliquots were reacted with 6 mM DTNB. All three samples were left in the dark for 20 min, and absorbances were then read in a Perkin–Elmer model Lambda 3B spectrophotometer at wavelength 412 nm. The NEM-treated value for each sample was subtracted from the corresponding DTNB samples. Absorbances obtained were then multiplied by the appropriate extinction coefficient and dilution factors, and values were calculated as nanomoles Pr-SH per $10^6$ cells.

$Ca^{2+}$ *determination.* Intracellular calcium concentrations were determined using the fluorescent dye indo-1AM. Aliquots of $10^6$ cells/mL were removed from $INO_2$-treated, stirred suspensions and washed in loading medium (serum free HEPES-medium without bicarbonate). Samples were then resuspended in 1 mL loading medium, and 50 $\mu$M verapamil was added in order to inhibit P-glycoprotein activity. Inhibition of P-glycoprotein on CHO cells was crucial for this assay because the fluorescent dye used for intracellular $Ca^{2+}$ determination, indo-1AM, has been shown previously to be a substrate for P-glycoprotein* and use of verapamil resulted in higher and more reproducible loading levels of indo-1AM. Though verapamil is noted for being a voltage-gated (Class II) $Ca^{2+}$ channel inhibitor, this voltage-sensitive channel is considered not to be constitutively expressed or active in cultured non-muscle cells such as CHO cells [20]. In addition, P-glycoprotein inhibition by

*Brezden CB, unpublished work.

verapamil has been shown previously to be exclusive from its effect on intracellular $Ca^{2+}$ levels [21]. Following a 10-min incubation with verapamil, 3 μM indo-1AM was added, and the samples were then incubated for 30 min at 37°. After this incubation period, samples were centrifuged (1300 *g* for 1 min), and the pellet was resuspended in $Ca^{2+}$ reading buffer containing: 1 mM $CaCl_2$, 140 mM NaCl, 5 mM KCl, 10 mM $Na^+$-HEPES (free acid), 10 mM glucose, pH 7.35. Fluorescence measurements were performed using a Perkin–Elmer model LS-3 spectrofluorometer with excitation at 355 nm and emission at 405 nm. The solution was maintained at 37° and stirred continuously. Ionomycin and $MnCl_2$ were used to calibrate the assay, and the intracellular $Ca^{2+}$ concentration was calculated as previously described by Grynkiewicz *et al.* [22].

*Cell preparation for electron microscopy.* Following a 1-hr exposure to 40 mM $INO_2$ under hypoxic conditions, or 45 μM INO treatment under aerobic conditions for 30 min, cell samples containing $10^6$ cells/mL were washed once in PBS and prepared for both transmission and scanning electron microscopy. For transmission electron microscopy, cells ($10^6$ cells/mL) were resuspended and fixed in 2.5% glutaraldehyde solution (prepared in PBS) at room temperature. The sample was then centrifuged and the pellet was washed twice with PBS. Post-fixation of the sample was in 1% osmium tetroxide (prepared in PBS) for 1 hr followed by two rinses in distilled water. Dehydration of the sample in a series of ethanol rinses was carried out, and the sample was then resuspended in a propylene oxide/epon mix and allowed to dessicate and polymerize. The polymerized sample was then sectioned on a microtome and prepared for transmission electron microscopy. For scanning electron microscopy, a washed droplet of cells (in PBS) was placed on a poly-L-lysine-treated glass coverslip for 30 min prior to fixation in 2.5% glutaraldehyde. The coverslip was then dehydrated in a series of ethanol rinses followed by critical point drying. Coverslips were then mounted and coated with a gold-palladium mixture for scanning electron microscopy.

*DNA gel electrophoresis.* DNA from $INO_2$-treated CHO cells or IL-2-depleted CTLL-2 cells was isolated as previously described by Cumano *et al.* [23] with a few modifications. Briefly, 1-mL aliquots containing $10^6$ cells were removed for DNA extraction. Cells were washed initially with PBS and then microcentrifuged for 15 sec at 8000 *g* at room temperature. The supernatant was removed, the cell pellet was resuspended in 200 μL of 5 M GT (supplemented with 100 mM 2-mercaptoethanol), and the sample was vortexed vigorously. To this 200-μL GT sample, 7.5 M ammonium acetate, 20 mg/mL glycogen and 600 μL of 100% ethanol were added, and the sample was then vortexed and precipitated at −20° overnight. Following this, the sample was centrifuged for 30 min at high speed (8000 *g*) at −4°. The supernatant was carefully removed and washed twice with 75% ethanol. The pellet was air-dried and dissolved in Tris-EDTA (pH 8.0) buffer. Finally, RNase (20 μg/mL) was added, vortexed lightly, and allowed to incubate for 30 min at 37°. The DNA was electrophoresed on a 2.5% agarose gel prestained with ethidium bromide (0.6 μg/mL) at 80 V for 4 hr. DNA size markers λ*Hind* III and φx were run concurrently on each gel. Another protocol that isolated only the DNA fragments was also employed to verify the sensitivity of nucleosomal ladder detection using gel electrophoresis. This protocol was followed as previously described [24].

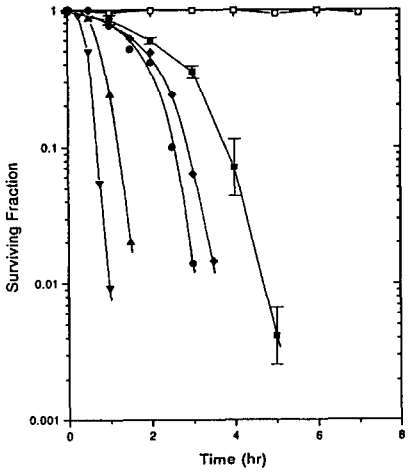


Fig. 1. Cell survival following hypoxic exposure to various concentrations of $INO_2$. Results display CHO cell survival at (■) 2.5 mM, (◆) 5 mM, (●) 10 mM, (▲) 20 mM, (▼) 40 mM, and (□) 40 mM (aerobic) $INO_2$ that occurred in both a concentration- and time-dependent manner. Values are an average of N = 3 experiments. For clarity SEM are shown only for the 2.5 mM $INO_2$ survival curve. These errors are representative for the other 5 curves.

## RESULTS

*$INO_2$ selective hypoxic cytotoxicity.* Various concentrations of $INO_2$ were incubated with CHO cells either under hypoxic or aerobic conditions. Figure 1 illustrates selective hypoxic cytotoxicity of $INO_2$ which was both concentration and time dependent. Moreover, it was evident that this dependency was not a simple concentration and time relationship since doubling the $INO_2$ concentration from 5 to 10 mM or from 20 to 40 mM did not halve the time to induce cytotoxicity under hypoxic conditions (Fig. 1). This result has been seen independently by others using the same cells.* In contrast, concurrent aerobic $INO_2$ treatment at the same concentrations did not show any significant cytotoxicity even up to 7 hr at a 40 mM drug concentration. This was consistent with a reduced degree of drug activation due to the inhibition by oxygen at the one electron reduction stage.

*Effect of $INO_2$ on intracellular GSH levels.* When $INO_2$ was added to hypoxic cells at 2.5, 10 and 40 mM concentrations, GSH depletion was observed to be both concentration and time dependent (Fig.

*Bérubé L, personal communication. Cited with permission.

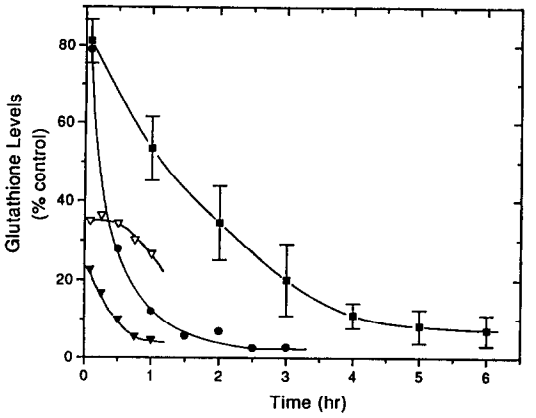


Fig. 2. Glutathione levels in CHO cells following $INO_2$ hypoxic exposure at (■) 2.5 mM, (●) 10 mM, (▼) 40 mM, and (▽) 40 mM (aerobic) $INO_2$. Values are expressed as percent of control, where control values (samples with no drug) were measured concurrently with the drug-treated samples. Values are an average of N = 3 experiments, and errors shown only on the 2.5 mM data (for clarity) represent SEM. The GSH level taken as 100% was 6.3 ± 0.4 nmol/$10^6$ cells (±SEM).

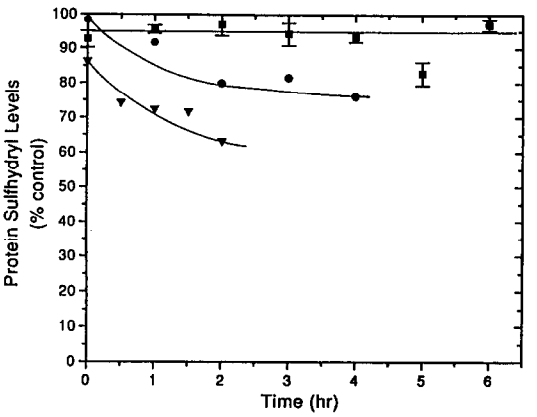


Fig. 3. Protein sulfhydryl levels in CHO cells following hypoxic exposure at (■) 2.5 mM, (●) 10 mM, and (▼) 40 mM $INO_2$. Values are expressed as percent of control, where control values (samples with no drug) were measured concurrently with the drug-treated samples. Values are an average of N = 3 experiments, and errors shown only on the 2.5 mM data (for clarity) represent SEM. The Pr-SH level taken as 100% was 24.7 ± 0.4 nmol/$10^6$ cells (±SEM).

2). At the shortest time measured, within 1 min after 2.5 or 10 mM $INO_2$ addition, there was a significant degree of GSH depletion (20%). This was even more notable at the 40 mM drug concentration level. This rapid depletion was not due to a direct reaction of high concentrations of $INO_2$ with GSH or an inhibitory effect of $INO_2$ on the Tietze assay (data not shown). GSH levels were not depleted completely, suggesting that access or activation of the drug in some areas of the cell, such as within the mitochondrion [25], may be limited and account for the remaining 2–10% GSH. GSH depletion was correlated with $INO_2$ cytotoxicity under hypoxic conditions (Fig. 1) for 2.5, 10 and 40 mM $INO_2$, since the degree of GSH depletion for equitoxic drug levels was similar for the 16-fold range of drug concentrations. Significant cell killing was seen at GSH levels below 20% of control levels, suggesting that GSH depletion may be one factor responsible for this selective hypoxic cytotoxicity of $INO_2$. Incubation of cells with $INO_2$ under aerobic conditions at the concentrations employed above did not result in such a drastic GSH depletion, although initial reductions in GSH levels of up to 65% were observed at the highest drug concentration of 40 mM (Fig. 2) but with no evidence of cytotoxicity. This immediate GSH depletion may be a direct result of redox cycling of the drug at such a high concentration.

*Effect of $INO_2$ on intracellular Pr-SH levels.* The same concentrations of $INO_2$ used for measuring GSH depletion were investigated for their effects on total Pr-SH within the cell. Incubation of cells with 2.5, 10 or 40 mM $INO_2$ revealed maximum depletions of 5, 25 and 40%, respectively; however, the 2.5 mM $INO_2$ results were not significantly different from the control (Fig. 3). This latter result may suggest that the cells are capable of repairing damage to Pr-SH resulting from $INO_2$ hypoxic metabolism. There

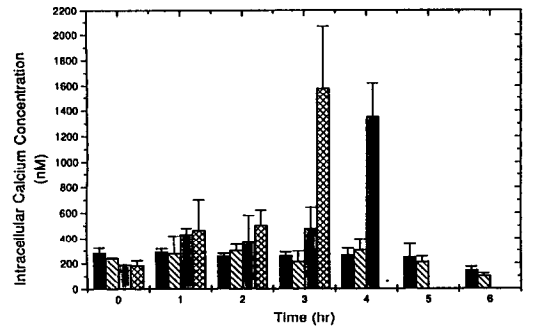


Fig. 4. Intracellular calcium levels measured in CHO cells following $INO_2$ hypoxic exposure at (▨) 2.5 mM, (▨) 10 mM, (▨) 40 mM, and (■) control (no drug). Time intervals studied for the above drug concentrations correspond to the concentration–time dependent cytotoxicity (see Fig. 1). Values are an average of N = 3 experiments, and errors shown represent SEM.

was not as good a correlation between Pr-SH depletion (Fig. 3) and hypoxic toxicity (Fig. 1) as seen for GSH depletion. Different mechanisms of toxicity may be involved at low and high drug concentrations. Aerobic incubation at 2.5, 10 and 40 mM $INO_2$ did not reveal any significant changes in Pr-SH levels (data not shown), once again suggesting that $INO_2$ hypoxic bioreduction is imperative for extensive thiol depletion.

*Effect of $INO_2$ on $Ca^{2+}$ homeostasis.* Since $INO_2$ treatment caused an altered cellular redox state under hypoxic conditions, it was of interest to study intracellular $Ca^{2+}$ levels during drug incubation. Furthermore, Bérubé *et al.* [13] showed that INO

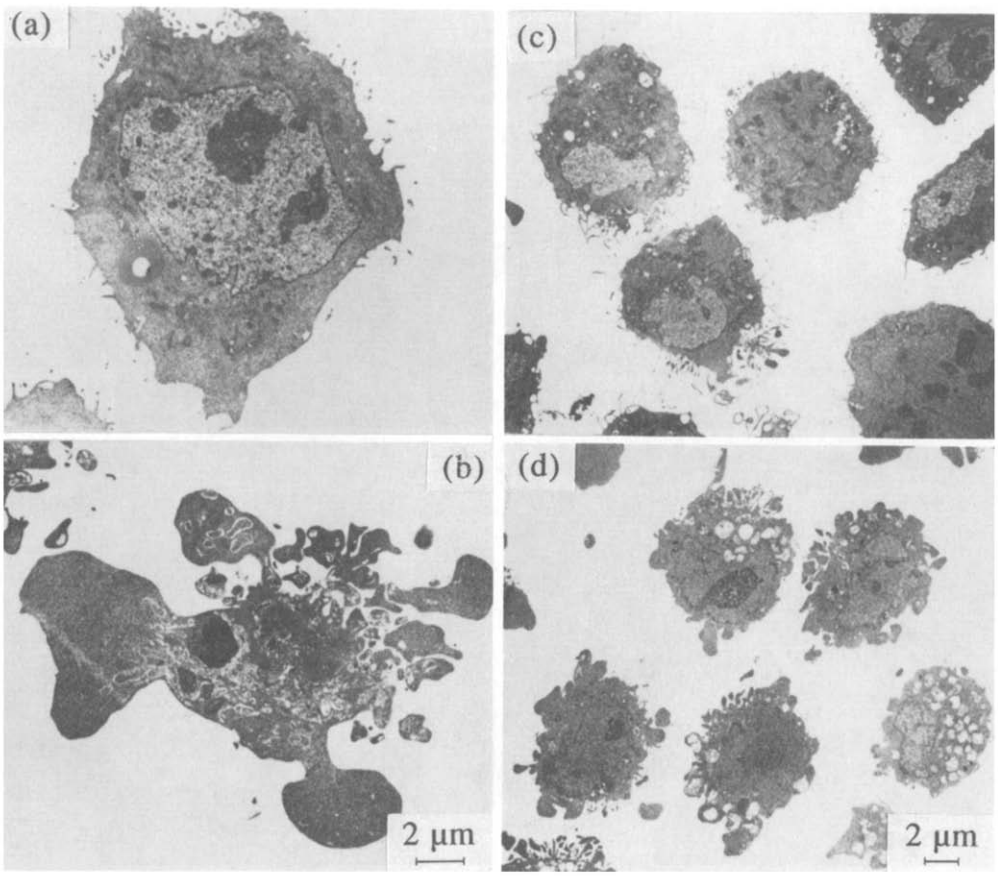


Fig. 5. Transmission electron microscopy of CHO cells assayed following a 1-hr hypoxic treatment with no drug (hypoxic control) [a] and 40 mM $INO_2$ [b]; and aerobic exposure following 30 min with no drug (control) [c] and 45 $\mu$M INO [d]. Approximately 90% of all drug-treated cells were undergoing the above morphological perturbations of membrane blebbing, chromatin condensation and organelle compaction, typical of cells undergoing apoptosis. Further inspection of the apoptotic bodies (blebs) revealed that they contained some degraded DNA, free ribosomes and intact organelles.

treatment resulted in a sustained elevation of intracellular $Ca^{2+}$ at INO concentrations that were toxic to the cell. Figure 4 illustrates intracellular $Ca^{2+}$ levels following 2.5, 10, and 40 mM $INO_2$ treatment under hypoxic conditions along with control values. At increasing $INO_2$ concentrations (10 and 40 mM), a rise in intracellular $Ca^{2+}$ levels to values 3 to 8-fold higher than control was observed at 3–4 hr; however, there was no change with 2.5 mM $INO_2$ incubation up to 6 hr, the longest time studied. Aerobic $INO_2$ treatment at the above concentrations and time periods did not perturb intracellular $Ca^{2+}$ levels (data not shown), suggesting that reductive species of $INO_2$, generated under hypoxia, could cause such effects. A sustained rise in the intracellular $Ca^{2+}$ concentration may result in the activation of $Ca^{2+}$-dependent catabolic enzymes (proteases, phospholipases, endonucleases) that can be detrimental to the cell.

*Effect of $INO_2$ on cellular morphology.* Treatment of hypoxic cells with $INO_2$ resulted in thiol depletion and $Ca^{2+}$ elevation in a manner analogous to INO treatment [13]. Since the kinetics of both GSH and Pr-SH depletion and $Ca^{2+}$ increase were similar for the highest concentration of $INO_2$ (40 mM) compared with the previous results for INO at 45 $\mu$M, these two concentrations were used to study cell morphology via electron microscopy. Figure 5 illustrates transmission micrographs of CHO cells treated for 60 min with 40 mM $INO_2$ under hypoxic conditions (Fig. 5b) and 30 min after 45 $\mu$M INO treatment (Fig. 5d) along with corresponding controls for the above treatments. It is evident from Fig. 5b that following a 1-hr hypoxic exposure to 40 mM $INO_2$, cellular morphology drastically changed as compared with the control population (Fig. 5a): transmission micrographs of 40 mM $INO_2$-treated CHO cells revealed plasma membrane blebbing (zeiosis), cell and nuclear shrinkage, chromatin condensation and organelle compaction with organelle membrane integrity maintained. Scanning micrographs displayed loss of microvilli and extreme membrane blebbing or "boiling of the cytoplasm" (Fig. 6). Such perturbations of cellular morphology

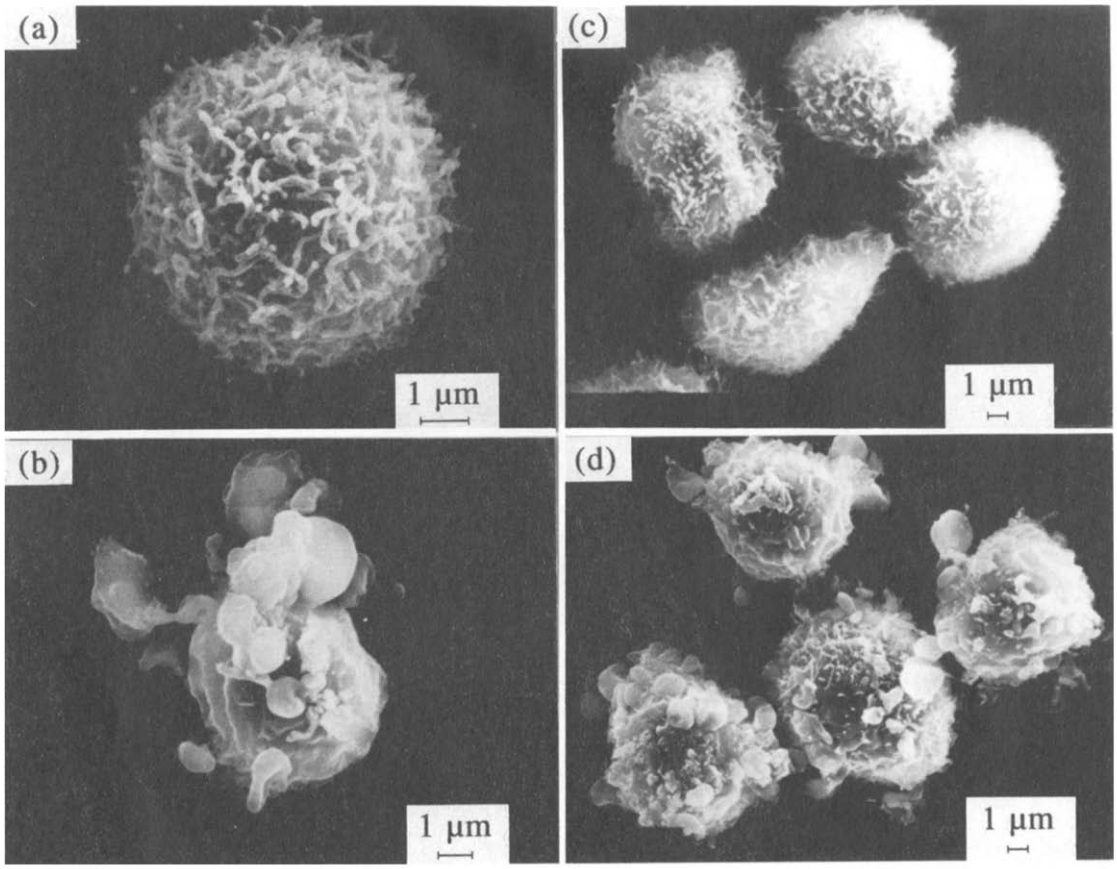


Fig. 6. Scanning electron microscopy of CHO cells assayed following a 1-hr hypoxic treatment with no drug (hypoxic control) [a] and 40 mM $INO_2$ [b]; and aerobic exposure following 30 min with no drug (control) [c] and 45 μM INO [d]. Control populations ([a] and [c]) displayed spherical cells with surface microvilli, whereas drug-treated cells ([b] and [d]) showed drastic membrane blebbing ("boiling of the cytoplasm") with loss of microvilli. Approximately 90% of drug-treated cells were undergoing the apoptotic morphological perturbations shown above.

were present in 80–90% of both 45 μM INO- and 40 mM $INO_2$-treated cells under aerobic and hypoxic conditions, respectively. Furthermore, trypan blue staining at the time of microscopy (30 min after 45 μM INO and 1 hr following 40 mM $INO_2$ treatment) showed no stain uptake by the blebbed cells (data not shown), indicating that the plasma membrane was still intact. The above observations of altered cellular morphology are characteristic of cells undergoing an apoptotic cell death [25].

*$INO_2$ and DNA gel electrophoresis.* Since both 40 mM hypoxic $INO_2$ and 45 μM aerobic INO cellular treatments resulted in morphological features of cells undergoing apoptosis, total DNA was isolated from these treated cells in order to determine whether DNA ladders were present. Figure 7 illustrates a DNA gel from CHO cells exposed for various lengths of time to 40 mM $INO_2$ (hypoxic conditions). A cytotoxic T lymphocytic cell line (CTLL-2) was used as a positive control for the protocol. CTLL-2 cells were deprived of IL-2 for a period of 14 hr. Figure 7 displays this DNA ladder from CTLL-2 IL-2-deprived cells along with DNA isolated from $INO_2$-treated CHO cells at the times indicated. It is evident that DNA ladders were not observed in cells treated with 40 mM $INO_2$ (hypoxic) at the times studied. Similar negative results were obtained for INO-treated cells (data not shown). A possible explanation for the failure to observe DNA ladders could be attributed to the sensitivity of the assay applied for DNA fragment detection. Another protocol that isolated only fragmented DNA was therefore employed (see Ref. 24) with the above treatment conditions, but ladders were still not observed in CHO cells; however, IL-2-deprived CTLL-2 cells did reveal the characteristic apoptotic DNA ladder (data not shown).

## DISCUSSION

There is good evidence to support the proposal that bioreduction of the nitro moiety of 2-nitroimidazoles results in formation of reactive intermediate species that are implicated in selective hypoxic cytotoxicity, neurotoxicity, and chemosensitization [26–28]. Djuric [29] suggested that a

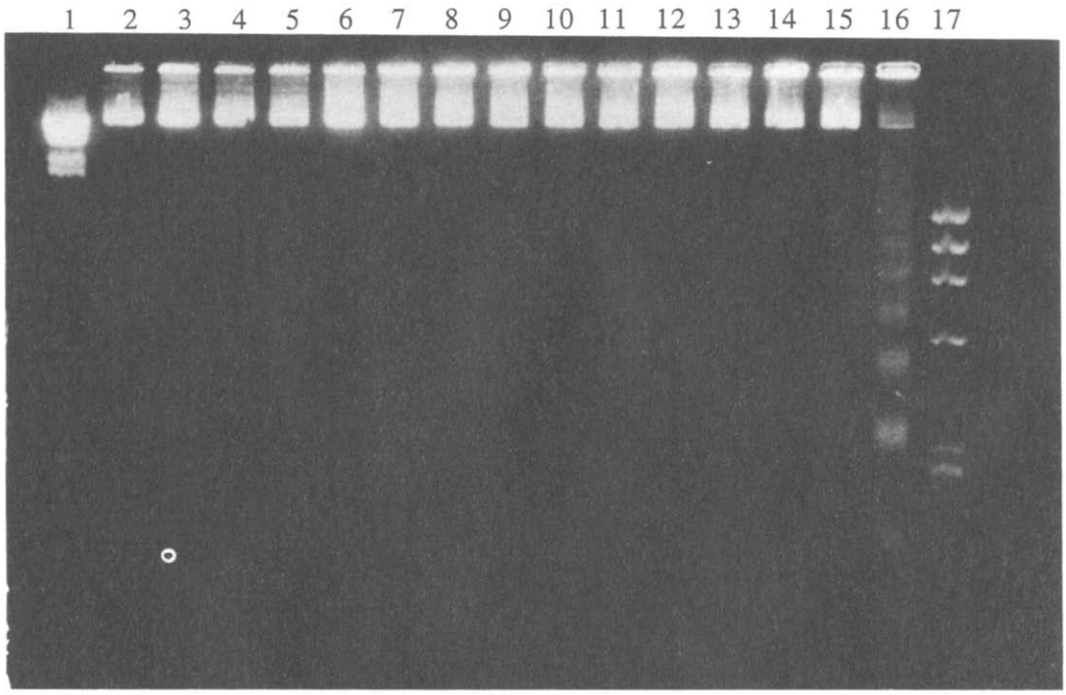


Fig. 7. Gel electrophoresis of DNA from control CHO cells and CHO cells following treatment with 40 mM $INO_2$ for the times indicated as follows: Lanes 1 and 17 show DNA markers $\lambda$*Hin*dIII and $\phi\chi$, respectively; Lanes 2, 4, 6, 8, 10, 12, and 14 display DNA from control CHO cells at times 0, 15, 30, 45, 60, 90 and 120 min following hypoxic treatment, respectively; Lanes 3, 5, 7, 9, 11, 13, and 15 display DNA isolated from 40 mM $INO_2$-treated CHO cells at times 0, 15, 30, 45, 60, 90 and 120 min following hypoxic drug treatment, respectively. Lane 16 is DNA isolated from CTLL-2 cells deprived of IL-2 for 14 hr. Drug-treated cells did not reveal any DNA ladders, whereas the IL-2-deprived CTLL-2 cells did display the characteristic DNA ladder of cells undergoing apoptosis.

possible mechanism for the cytotoxicity of MISO was the formation of reductive intermediates that bind to DNA and induce lethal strand breaks. In fact, DNA damage induced by reduced nitroimidazoles has been considered to be the primary cause leading to cell death [30–32]. These studies provided a biochemical understanding of the DNA adducts formed when 2-nitroimidazoles were reduced either chemically or enzymatically in cell-free systems. However, these examples of DNA interaction with reduced MISO do not differentiate whether DNA binding is the primary cause of cell death or simply an effect due to interactions with other cellular targets (e.g. intracellular thiols).

Raleigh and Koch [33] demonstrated the importance of intracellular thiols in the reductive binding of 2-nitroimidazoles to cellular protein rather than to DNA. It was observed by Cline *et al.* [34] that reduced 2-nitroimidazole binding was concentrated in the cytoplasm of cells of spontaneous canine tumours. Hence, cytoplasmic reduction of 2-nitroimidazoles may occur with cellular proteins being the primary target for cytotoxicity with the possible diffusion of these reactive intermediates into the nucleus for further binding to DNA. It was therefore of interest to study cellular reactions of 2-nitroimidazoles under both hypoxic and aerobic conditions by using $INO_2$ as a model. Furthermore, data on the reactivity of the $2e^-$ reduction product of $INO_2$, the nitroso (INO), was available for comparison with data generated with $INO_2$ [13].

Selective hypoxic cytotoxicity to CHO cells was observed with $INO_2$, which occurred in a concentration- and time-dependent manner but not by a simple concentration–time relationship (Fig. 1). In addition, $INO_2$ depleted intracellular GSH levels by greater than 90% selectively under hypoxic conditions. This depletion was correlated with cell killing (Fig. 2), and this depletion was similar to what was observed previously with the INO intermediate at equitoxic concentrations [11]. It has been shown that chemically reduced MISO can form stable GSH conjugates that may be responsible for intracellular GSH depletion [35]. INO can react chemically with excess GSH in a cell-free system to form INO:GSH adducts in a 1:3 stoichiometric reaction [36]. The kinetics of depletion were slower following $INO_2$ hypoxic treatment than observed for INO, since $INO_2$ has to be reduced to a toxic species, presumably INO, in order to react with and deplete GSH. Depletion of GSH was approximately 90% for both hypoxic $INO_2$ treatment and aerobic INO treatment, consistent with INO being the reductive species responsible for the observed GSH depletion.

GSH is the most abundant non-protein thiol and plays a very important role in cellular detoxification

of harmful xenobiotics [37]. This ubiquitous tripeptide also plays a pivotal role in many physiological processes including cellular redox state, enzyme activity and maintenance, microtubule assembly and cytoskeletal structure, mixed disulfide exchange and neurotransmitter release from axonal endings [37]. GSH has also been shown to provide cellular radioprotection against ionizing radiation [38]. Therefore, depletion of this very important molecule could have serious consequences to cellular processes, especially those dependent on a balanced redox state.

Pr-SH levels were also depleted with higher concentrations of $INO_2$ preferentially under hypoxic conditions as was seen previously with INO treatment [13]. Pr-SH exist at a 10-fold higher concentration than GSH in the cell, and depletion either through mixed disulfide exchange or as a result of inter- or intra-protein disulfide bridges may lead to an impairment of normal protein function that is dependent on reduced thiol configurations [14]. These functions may include proteins whose enzymatic activity depends on key SH groups. Such a critical role of protein SH groups for enzymatic activity was demonstrated by Bellomo *et al.* [39], who showed that oxidation of key SH groups located on ATP-dependent $Ca^{2+}$ translocases may contribute to perturbations of $Ca^{2+}$ homeostasis during oxidative stress. In fact, following hypoxic treatment with $INO_2$ at concentrations that depleted Pr-SH levels, intracellular $Ca^{2+}$ levels increased to values considered lethal to the cell (Fig. 4). This observation was similar to that seen with INO treatment [13], suggesting that INO is the toxic reductive species of $INO_2$.

Mirabelli *et al.* [40, 41] have also shown that thiol depletion by the redox-active quinone menadione results in perturbations in cytoskeletal integrity. These alterations in membrane morphology were shown to be due to the oxidation of critical thiol groups in the cytoskeletal protein actin, which resulted in plasma membrane blebbing. Furthermore, disturbances in intracellular thiol and $Ca^{2+}$ homeostasis have been suggested as the mechanism responsible for plasma membrane bleb formation in hepatocytes [42]. These morphological perturbations, or membrane blebs, along with increases in intracellular $Ca^{2+}$ levels are two characteristic features of cells undergoing an apoptotic cell death [25].

Apoptosis or "programmed cell death" was first characterized by Wyllie, Kerr and Currie who described two modes of cell death: apoptosis and necrosis [25]. Apoptosis differs from necrosis both morphologically and biochemically. Morphological changes in apoptosis involve cell shrinkage, chromatin condensation, maintenance of normal organelle structure, organelle compaction and plasma membrane blebbing (zeiosis). Necrotic or "accidental cell death" is characterized by cell swelling with plasma and organelle membrane rupture, resulting in a total loss of organized cellular structure. Biochemically, necrotic cells display loss of osmoregulation that leads to the observed cell swelling and random DNA digestion by non-specific lysosomal enzymes released from ruptured lysosomes. In contrast, apoptotic cells demonstrate specific DNA digestion due to the action of endogenous endonucleases that are activated either by elevated levels of $Ca^{2+}$ [43] or decreased intracellular pH [44]. When electrophoretic separation is performed on DNA isolated from cells undergoing programmed cell death, a very distinct band pattern or "ladder" is observed. This DNA ladder consists of oligonucleosomal fragments that are multiples of 200 base pairs resulting from endonucleolytic cleavage at specific nucleosomal sites on the DNA.

Both $INO_2$ (hypoxic) and INO (aerobic) treated CHO cells revealed extensive membrane blebbing with additional features characteristic of apoptotic cells when observed under electron microscopy (Figs. 5 and 6). These features included cell and nuclear shrinkage, organelle compaction, chromatin condensation, and maintenance of organelle and plasma membrane integrity (measured by trypan blue exclusion) with loss of surface microvilli. Also, upon further observation of the micrographs, it was noted that the apoptotic bodies (blebs) contained ribosomes, intact organelles and some degraded chromatin. However, further analysis of DNA isolated from cells treated with 40 mM $INO_2$ did not reveal the characteristic DNA ladders up to 2 hr after treatment (Fig. 7). Even longer times of incubation, 2–72 hr after drug exposure, failed to show any evidence of DNA ladders (data not shown). However, the morphological effects evidenced by $INO_2$ are consistent with previous data showing that MISO induced hypoxic specific membrane blebbing of Chinese hamster V79 cells [45]. The biochemical feature of increased intracellular $Ca^{2+}$, which has been shown to activate endogenous endonucleases of apoptotic cells [43], and the morphological features of both $INO_2$- and INO-treated cells were consistent with cells dying apoptotically. It is important to note that examples showing nucleosomal ladders represent extreme cases of DNA fragmentation, where most if not all DNA is cleaved and therefore can be detected with gel electrophoresis. Digestion of all the cellular DNA is not required for cell death [46]. Hence, in cases where internucleosomal digestion of DNA is not observed, as in the present case, the cells may still be undergoing apoptosis with only a minimal fraction of genomic DNA being fragmented. It should therefore not be discredited that following $INO_2$ treatment under hypoxic conditions, morphological and biochemical changes typical of apoptotic cells are occurring, even though DNA ladders are not detected [47]. Perhaps more sensitive flow cytometric techniques that quantitate the amounts of degraded DNA would detect DNA fragmentation following both $INO_2$ and INO exposure. The dependence of blebbing and intracellular $Ca^{2+}$ levels on protein synthesis following both $INO_2$ and INO exposure could be evaluated with cycloheximide and actinomycin D treatment to further test the apoptosis model.

In conclusion, the present paper addresses the underlying factors responsible for the cytotoxic effects of reduced 2-nitroimidazoles by using $INO_2$ as a model. It provides evidence consistent with the $2e^-$ reduction product of $INO_2$, the INO derivative

being the toxic reductive species mediating $INO_2$ selective hypoxic cytotoxicity. Cytotoxic effects involved in the action of reduced $INO_2$ were shown to cause perturbations in intracellular thiol and $Ca^{2+}$ homeostasis as well as alterations in cellular morphology. These alterations in $Ca^{2+}$ levels and cell morphology are characteristic features of cells dying apoptotically. Hence, $INO_2$ selective hypoxic cytotoxicity is similar to that mediated through the $2e^-$ reduction product added directly to cells, which also affects cellular homeostasis and mediates cell death through an apoptotic-like death mechanism. By further understanding the mechanism involved in 2-nitroimidazole selective hypoxic cytotoxicity, procedures may be implemented to target these agents more selectively to neoplastic cells and thereby decrease normal tissue toxicity, such as the peripheral neuropathy experienced by patients receiving 2-nitroimidazoles in combination with radiotherapy.

*Acknowledgements*—This work was supported by the Medical Research Council and the National Cancer Institute of Canada. Electron microscopy was conducted at the Max Bell Research Centre, University of Toronto, under the direction of Dr. E. DeHarven.

## REFERENCES

1. Thomlinson RH and Gray LH, The histological structure of some human lung cancers and the possible implications for radiotherapy. *Br J Cancer* **9**: 539–549, 1955.
2. Coleman CN, Wasserman TH, Urtasun RC, Halsey J, Noll L, Hancock S and Phillips TL, Final report of the Phase I trial of the hypoxic cell radiosensitizer SR-2508 (etanidazole): Radiation Therapy Oncology Group 83-03. *Int J Radiat Oncol Biol Phys* **18**: 389–393, 1990.
3. Wasserman TH, Lee DJ, Cosmatos D, Coleman N, Phillips T, Davis L, Marcial V and Stetz J, Clinical trials with etanidazole (SR-2508) by the radiation therapy oncology group (RTOG). *Radiother Oncol* **S20**: 129–135, 1991.
4. Bleehen NM, Maughan TS, Workman P, Newman HFV, Stenning S and Ward R, The combination of multiple doses of etanidazole and pimonidazole in 48 patients: A toxicity and pharmacokinetic study. *Radiother Oncol* **S20**: 137–142, 1991.
5. Chassagne D, Sancho-Garnier H, Charreau I, Eschwege F and Malaise EP, Progress report of a Phase II and a Phase III trial with etanidazole (SR-2508): A multicentre European study. *Radiother Oncol* **S20**: 121–127, 1991.
6. Rasey JS, Koh WJ, Griersen JR, Greenbaum Z and Krohn KA, Radiolabelled fluoromisonidazole as an imaging agent for tumor hypoxia. *Int J Radiat Oncol Biol Phys* **17**: 985–991, 1989.
7. Prekeges JL, Rasey JS, Greenbaum Z and Krohn KA, Reduction of fluoromisonidazole, a new imaging agent for hypoxia. *Biochem Pharmacol* **42**: 2387–2395, 1991.
8. Varghese AJ and Whitmore GF, Binding of nitro-reduction products of misonidazole to nucleic acids and proteins. *Cancer Clin Trials* **3**: 43–46, 1980.
9. Varghese AJ and Whitmore GF, Binding to cellular macromolecules as a possible mechanism for the cytotoxicity of misonidazole. *Cancer Res* **40**: 2165–2169, 1980.
10. McClelland RA, Fuller JR, Seaman NE, Rauth AM and Battistella R, 2-Hydroxylaminoimidazoles—unstable intermediates in the reduction of 2-nitroimidazoles. *Biochem Pharmacol* **33**: 303–309, 1984.
11. Noss MB, Panicucci R, McClelland RA and Rauth AM, Preparation, toxicity and mutagenicity of 1-methyl-2-nitrosoimidazole. A toxic 2-nitroimidazole reduction product. *Biochem Pharmacol* **37**: 2585–2593, 1988.
12. Gipp JJ, McClelland RA and Mulcahy RT, DNA damage induced in HT-29 colon cancer cells by exposure to 1-methyl-2-nitrosoimidazole, a reductive metabolite of 1-methyl-2-nitroimidazole. *Biochem Pharmacol* **42**: S127–S133, 1991.
13. Bérubé LR, Farah S, McClelland RA and Rauth AM, Effect of 1-methyl-2-nitrosoimidazole on intracellular thiols and calcium levels in Chinese hamster ovary cells. *Biochem Pharmacol* **42**: 2153–2161, 1991.
14. Gilbert HF, Redox control of enzyme activities by thiol/disulfide exchange. *Methods Enzymol* **107**: 330–351, 1984.
15. McClelland RA, Panicucci R and Rauth AM, Products of the reduction of 2-nitroimidazoles. *J Am Chem Soc* **109**: 4308–4311, 1987.
16. Karasuyama H, Tohyama N and Tada T, Autocrine growth and tumorigenicity of interleukin-2-dependent helper T cells transfected with IL-2 gene. *J Exp Med* **169**: 13–25, 1989.
17. Tietze F, Enzymic method for quantitative determination of nanogram amounts of total and oxidized glutathione: Applications to mammalian blood and other tissues. *Anal Biochem* **27**: 502–522, 1969.
18. Bump EA, Taylor YC and Brown JM, Role of glutathione in the hypoxic cell cytotoxicity of misonidazole. *Cancer Res* **43**: 997–1002, 1983.
19. Albano E, Rundgren M, Harvison PJ, Nelson SD and Moldéus P, Mechanisms of *N*-acetyl-*p*-benzoquinone imine cytotoxicity. *Mol Pharmacol* **28**: 306–311, 1985.
20. Cano-Gauci DF and Riordan JR, Action of calcium antagonists on multidrug resistant cells. Specific cytotoxicity independent of increased cancer drug accumulation. *Biochem Pharmacol* **36**: 2115–2123, 1987.
21. Nygren P and Larsson R, Verapamil and cyclosporin A sensitize human kidney tumor cells to vincristine in absence of membrane P-glycoprotein and without apparent changes in the cytoplasmic free calcium concentrations. *Biosci Rep* **10**: 231–237, 1990.
22. Grynkiewicz G, Poenie M and Tsien RY, A new generation of $Ca^{2+}$ indicators with greatly improved fluorescence properties. *J Biol Chem* **260**: 3440–3450, 1985.
23. Cumano A, Paige CJ, Iscove NN and Brady G, Bipotential precursors of B cells and macrophages in murine fetal liver. *Nature* **356**: 612–615, 1992.
24. Bissonnette RP, Echeverri F, Mahboubi A and Green DR, Apoptotic cell death induced by c-*myc* is inhibited by *bcl*-2. *Nature* **359**: 552–554, 1992.
25. Wyllie AH, Kerr JF and Currie AR, Cell death: The significance of apoptosis. *Int Rev Cytol* **68**: 251–306, 1980.
26. Walton MI and Workman P, Nitroimidazole bioreductive metabolism. Quantitation and characterisation of mouse tissue benznidazole nitroreductases *in vivo* and *in vitro*. *Biochem Pharmacol* **36**: 887–896, 1987.
27. Edwards DI, Knox RJ, Rawley DA, Skolimowski IM and Knight RC, Nitroimidazoles: Chemistry, pharmacology, and clinical applications. In: *Radiation Sensitizers* (Eds. Breccia A, Cavalleri B and Adams GE), pp. 105–112. Plenum Press, New York, 1982.
28. Rauth AM, Pharmacology and toxicology of sensitizers: Mechanism studies. *Int J Radiat Oncol Biol Phys* **10**: 1293–1300, 1984.
29. Djuric Z, Reductive metabolism and DNA binding of

misonidazole. *Toxicol Appl Pharmacol* **101**: 47–54, 1989.
30. Knox RJ, Knight RC and Edwards DI, Misonidazole-induced thymidine release from DNA. *Biochem Pharmacol* **30**: 1925–1929, 1981.
31. Silver ARJ, McNeil SS, O'Neill P, Jenkins TC and Ahmed I, Induction of DNA strand breaks by reduced nitroimidazoles: Implications for DNA base damage. *Biochem Pharmacol* **35**: 3923–3928, 1986.
32. Zahoor A, Lafleur VM, Knight RC, Laman H and Edwards DI, DNA damage induced by reduced nitroimidazole drugs. *Biochem Pharmacol* **36**: 3299–3304, 1987.
33. Raleigh JA and Koch CJ, Importance of thiols in the reductive binding of 2-nitroimidazoles to macromolecules. *Biochem Pharmacol* **40**: 2457–2464, 1990.
34. Cline JM, Thrall DE, Page RL, Franko AJ and Raleigh JA, Immunohistochemical detection of a hypoxia marker in spontaneous canine tumours. *Br J Cancer* **62**: 925–931, 1990.
35. Varghese AJ and Whitmore GF, Misonidazole–glutathione conjugates in Chinese hamster ovary cells. *Int J Radiat Oncol Biol Phys* **10**: 1341–1345, 1984.
36. Farah S, Aspects of the reduction of 1-methyl-2-nitroimidazole with glutathione and the reaction of 1-methyl-2-nitrosoimidazole with glutathione. *Ph.D. Thesis*, Department of Chemistry, University of Toronto, 1991.
37. Kosower NS and Kosower EM, The glutathione status of cells. *Int Rev Cytol* **54**: 109–160, 1978.
38. Bump EA and Brown JM, Role of glutathione in the radiation response of mammalian cells *in vitro* and *in vivo*. *Pharmacol Ther* **47**: 117–136, 1990.
39. Bellomo G, Mirabelli F, Richelmi P and Orrenius S, Critical role of sulfhydryl group(s) in ATP-dependent $Ca^{2+}$ sequestration by the plasma membrane fraction from rat liver. *FEBS Lett* **163**: 136–139, 1983.
40. Mirabelli F, Salis A, Marinoni V, Finardi G, Bellomo G, Thor H and Orrenius S, Menadione-induced bleb formation in hepatocytes is associated with the oxidation of thiol groups in actin. *Arch J Biochem Biophys* **264**: 261–269, 1988.
41. Mirabelli F, Salis A, Perotti M, Taddei F, Bellomo G and Orrenius S, Alterations of surface morphology caused by the metabolism of menadione in mammalian cells are associated with the oxidation of critical thiol groups in cytoskeletal proteins. *Biochem Pharmacol* **37**: 3423–3427, 1988.
42. Jewell SA, Bellomo G, Thor H, Orrenius S and Smith MT, Bleb formation in hepatocytes during drug metabolism is caused by disturbances in intracellular thiol and calcium ion homeostasis. *Science* **217**: 1257–1259, 1982.
43. Cohen JJ and Duke RC, Glucocorticoid activation of a calcium-dependent endonuclease in thymocyte nuclei leads to cell death. *J Immunol* **132**: 38–42, 1984.
44. Barry MA and Eastman A, Endonuclease activation during apoptosis: The role of cytosolic calcium and pH. *Biochem Biophys Res Commun* **186**: 782–789, 1992.
45. Roizin-Towle L, Roizin L, Hall EJ and Liu JC, Effects of misonidazole on the ultrastructure of mammalian cells cultured *in vitro*. In: *Radiation Sensitizers* (Ed. Brady LW), pp. 444–449. Masson Publishing, New York, 1981.
46. Eastman A and Barry MA, The origins of DNA breaks: A consequence of DNA damage, DNA repair or apoptosis? *Cancer Invest* **10**: 229–240, 1992.
47. Vaux DL, Toward an understanding of the molecular mechanisms of physiological cell death. *Proc Natl Acad Sci USA* **90**: 786–789, 1993.